An Observational Study of the Katabatic Wind Confluence Zone near Siple Coast, West Antarctica*

DAVID H. BROMWICH AND ZHONG LIU

Polar Meteorology Group, Byrd Polar Research Center and Atmospheric Sciences Program, The Ohio State University, Columbus, Ohio

(Manuscript received 9 August 1994, in final form 9 August 1995)

ABSTRACT

A month-long field program to study the springtime katabatic wind confluence zone (where katabatic winds converge) has been carried out near Siple Coast, West Antarctica. Based on previous observations and numerical studies, two surface camps, Upstream B (83.5°S, 136.1°W) and South Camp (84.5°S, 134.3°W), were established. Ground-based remote sensing equipment (sodar and RASS), along with conventional observations, were used. Combining the analyses of surface observations and wind and temperature profiles at the above camps, the following picture for the cross-sectional structure of the confluence zone emerges. A relatively cold katabatic airflow, which probably comes from East Antarctica, occupies the layer between the surface and roughly 500 m AGL. Low-level jets are present below 200 m AGL and are stronger near the Transantarctic Mountains. Diurnal variation is present in this cold drainage flow and decreases toward the Transantarctic Mountains. Weak-inversion-layer tops are found near 500 m AGL, which is roughly equal to the depth of the cold katabatic flow. The warmer West Antarctic katabatic airflow overlies the cold drainage flow from East Antarctica and has a depth of approximately 1000 m at Upstream B and more than 1500 m at South Camp; this is caused by blocking of the converging West Antarctic airflow by the Transantarctic Mountains. This warm flow originates near the surface far upslope in the vicinity of Byrd Station (80°S, 120°W). A baroclinic zone, formed where the two drainage flows are horizontally adjacent, appears to become unstable with some frequency to generate mesoscale cyclones.

1. Introduction

Numerical studies (Parish and Bromwich 1986, 1987, 1991; Parish et al. 1993; Gallée and Schayes 1994; Hines et al. 1995) have shown that katabatic winds are the most significant climatological feature of the boundary layer over Antarctica. The model results indicate that there are numerous confluence zones around the Antarctic periphery (Figs. 1, 2), where cold-air drainage currents from a large interior area converge. The resulting enhanced reservoirs of cold air feed coastal katabatic winds that as a result are stronger and more persistent. The summer streamline simulation by Parish and Bromwich (1986) (Fig. 3) resolves a confluence zone in the Siple Coast area. The 1984–85 and 1985–86 observational data (Bromwich 1986) taken at three temporary camps (geographic locations marked in Fig. 3) reveal several surface wind features: marked wind speed differences between these locations with highest wind speeds observed at South Camp (84.5°S, 134.3°W); and wind directional constancy (ratio of the magnitude of the mean wind vector to the mean wind speed) values increasing from north to south. It is known from observations in East Antarctica (Fig. 1), such as those at Cape Denison (Parish 1982) and Terra Nova Bay (Bromwich et al. 1993), that katabatic confluence zones are characterized by enhanced wind speeds and high directional constancies. These features indicate that South Camp resides in the confluence zone most of the time and that Upstream B (83.5°S, 136.1°W) sometimes does. These findings strongly support the summer wind field simulation of Parish and Bromwich (1986) (Fig. 3).

In comparison to the confluence zones over East Antarctica, the Siple Coast confluence zone offers a very different dynamical setting. First, terrain slopes are steeper in the interior than near the margins, and this leads to convergence of the airflow where terrain slopes become gentler rather than steeper. Second, the comparatively low elevation of West Antarctica allows the effects of synoptic disturbances to penetrate deep into the ice sheet interior. This, in combination with relatively gentle terrain slopes, may mean that Siple Coast winds are more affected by synoptic forcing than East Antarctic drainage flows. Third, the annual-mean potential temperature along the snow surface increases strongly with elevation (Radok 1973). By contrast, in East Antarctica, the potential temperature decreases

* Contribution 963 of Byrd Polar Research Center.

Corresponding author address: Dr. David H. Bromwich, Byrd Polar Research Center, Ohio State University, 1090 Carmack Road, 108 Scott Hall, Columbus, OH 43210-1002.

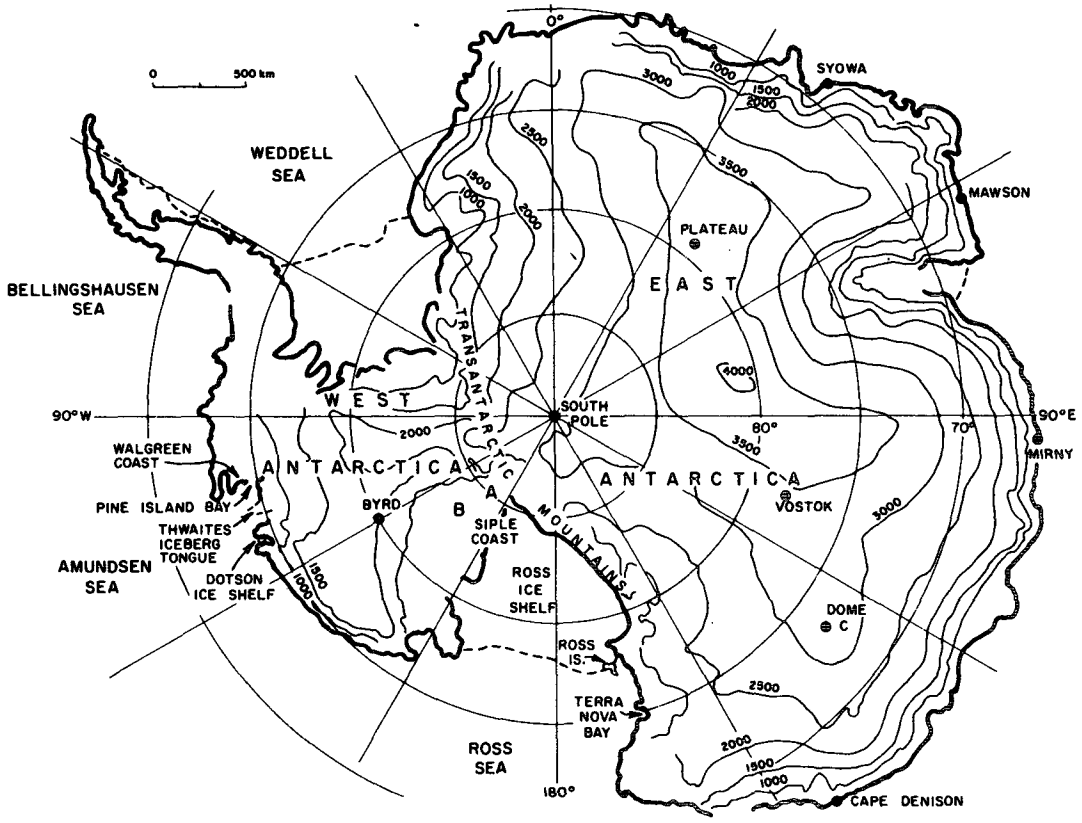

FIG. 1. Location of Siple Coast and other places mentioned in the text (from Parish and Bromwich 1986).

with elevation. This marked difference appears to imply very different atmospheric dynamics in the two areas (Radok 1973; Kodama and Wendler 1986; Stearns and Wendler 1988). Observational studies (Sorbjan et al. 1986; Wendler et al. 1988; Kodama et al. 1989) of the atmospheric boundary layer (ABL) in East Antarctica have been more extensive than in West Antarctica. In particular, there has been no observational study of the diurnal variations and vertical structure of the ABL in the Siple Coast confluence zone.

The 1992 spring field program was undertaken to further improve the understanding of this katabatic wind regime. Based upon the model results and previous surface observations (Bromwich 1986; Parish and Bromwich 1986), two sites (Upstream B and South Camp) for the campaign were chosen in the confluence zone near Siple Coast, West Antarctica (Fig. 3). An extensive observational network was established in order to study the confluence zone structure in both lateral and vertical directions. The present paper is organized as follows. Section 2 summarizes the instrumentation and data averaging. Sections 3 and 4 discuss the observed surface and ABL winds and temperatures. A synthesis is presented in section 5.

2. Sites, instrumentation, and data averaging

a. Sites and instrumentation

Elevations of the sites are 370 m at Upstream B and 666 m at South Camp (Fig. 4). These camps are nearly 110 km apart, and South Camp is approximately 100 km from the foot of the Transantarctic Mountains. The sun was continuously above the horizon at both sites. At South Camp, the topography was uniform, and the snow surface was hard with a well-developed sastrugi field. Sastrugi are defined by Schwerdtfeger (1984) as sharp, unyielding, irregular ridges formed on a snow surface by wind erosion and deposition. By contrast, the snow surface at Upstream B was soft and the sastrugi field was less well developed. The local terrain slopes are approximately 2.5×10^{-3} toward 285° at South Camp and 7×10^{-4} toward 260° at Upstream B, respectively.

Conventional surface observations, including wind, temperature, pressure, cloud type and amount, visibility, and weather, were taken at both sites at 3-h intervals (except 0300 and 0600 LST at South Camp and 0000, 0600, and 1800 LST at Upstream B from 11 November to 8 December 1992. Surface winds were continuously monitored by Lambrecht recording anemometers (periods: 22 November 1992–8 December

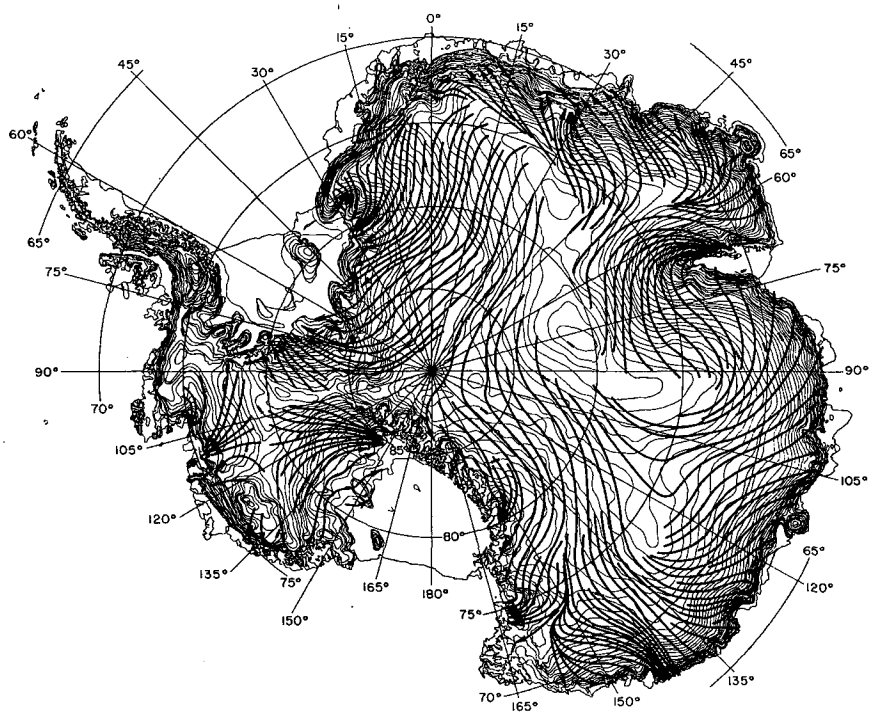

FIG. 2. Simulated streamlines (heavy lines) of time-averaged surface airflow over Antarctica (after Parish and Bromwich 1987). Thin lines are elevation contours in 100-m increments.

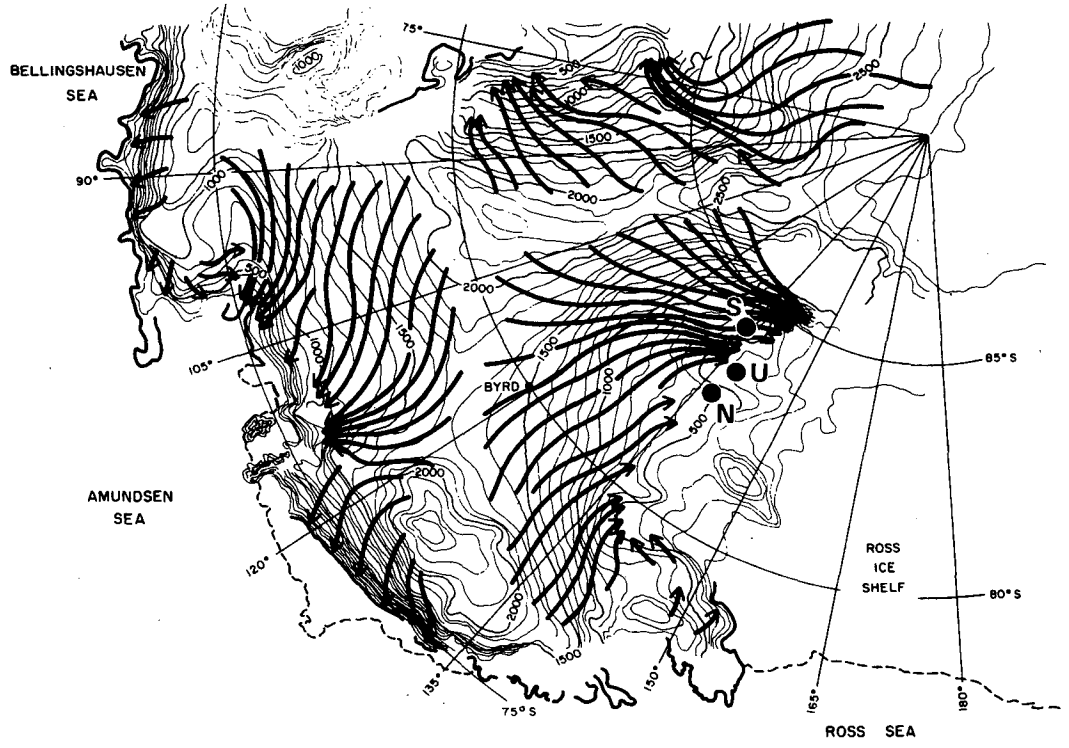

FIG. 3. Summer surface airflow (heavy lines) over the West Antarctic ice sheet (after Parish and Bromwich 1986). Thin lines are terrain contours in meters above sea level. The filled circles identify temporary camps occupied during the 1985–86 austral summer: "N" denotes North Camp, "U" indicates Upstream B camp, and "S" labels South Camp.

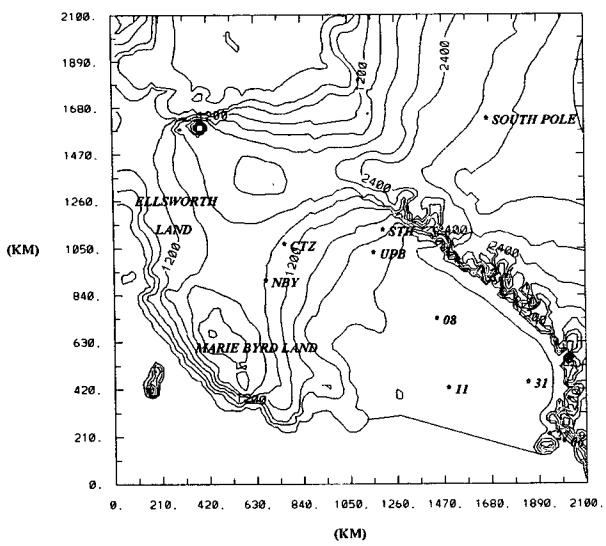

FIG. 4. Topographic map of West Antarctica. Stars marked with letters denote temporary camps. "UPB" denotes Upstream B, "STH" South Camp, "NBY" Byrd Camp, and "CTZ" Casertz Camp. Stars marked with numbers indicate automatic weather stations. Solid lines are elevation contours in 300-m increments.

1992 at Upstream B and 11 November 1992–8 December 1992 at South Camp). In addition, remote sensing profilers, sodar (sonic radar), and RASS (radio acoustic sounding system) were used. The accuracies for sodar and RASS are approximately 1.5 m s^{-1} and 1°C (May and Wilczak 1993). The sodar, which is three-axis and monostatic, was manufactured by Radian Corporation in Austin, Texas. It operates at an acoustic frequency of 2250 Hz and is capable of continuously profiling the boundary layer winds and backscatter. The sodar used in this campaign has 20 levels for winds and 200 levels for backscatter. The lowest level used was 35 m AGL (above ground level), and the vertical resolution was 50 m. The maximum measurable height was around 1000 m AGL. Detailed description of this sodar can be found in Liu and Bromwich (1993a).

Since 1975, several investigators (Hall and Owens 1975; Neff 1981; Mastrantonio et al. 1988; Argentini et al. 1992; Liu and Bromwich 1993a) have successfully deployed sodars for boundary layer studies in Antarctica. By contrast, RASS is relatively new to the Antarctic environment. RASS (also manufactured by Radian Corporation) used in this campaign was tested in 1991 at Williams Field near McMurdo Station, Antarctica, (Liu and Bromwich 1993b) and proved to be capable of continuously measuring temperature profiles in the boundary layer. RASS operates at 915 MHz. The lowest measurable level of the RASS was 85 m AGL and the vertical resolution was 75 m. Maximum measurable height varied from 500 to 900 m AGL. More detailed descriptions of RASS and the variation of maximum measurable height can be found in May and Wilczak (1993). Upstream B was equipped with a sodar and a RASS, while South Camp only had a RASS. Power for the sodar and RASS came from power generators at both camps. To minimize the effects of noise caused by power generators and vehicles, snow brick walls were built around the power generators to reduce the noise, and the sodar was situated about 100 m upwind. Due to the shortness of the RASS radar antenna cable, the RASS was situated several meters upwind from the power generator. RASS data show that the effect of noise from the power generator was undetectable. At South Camp, the only disturbances were those created by the two-man observational team. By contrast, near Upstream B, man-made obstacles (such as camp buildings) and vehicle noise were prevalent. To avoid these influences, the observational site was located about 1 km upwind from the base camp.

To overcome the maximum measurable height limit of both sodar and RASS, auxiliary balloon measurements were taken at both sites. The temperature, pressure, and humidity were measured with an Air-Sonde system developed by Atmospheric Instrumentation Research (AIR) in Boulder, Colorado. Air-Sonde launches were only taken at South Camp to provide details of the confluence zone structure. Pilot balloons were used at both camps to provide wind speed and direction. A summary of pilot balloon launches is given in Table 1.

Three-dimensional winds and backscatter data from the sodar were respectively recorded every 10 and 1 min. RASS temperature profiles were measured and stored on a hard disk twice per hour. Horizontal wind vector and wind speed averaging were used to produce composite analyses. A Lagrange interpolating polynomial (Burden and Faires 1985) was used to infer surface temperature data for hours when surface observations were not taken. The use of this interpolation method is based on the observed sinusoidal diurnal variation of surface temperature along the slope of Adélie Land, East Antarctica. To better understand the entire picture during the campaign, surface observational data recorded by U.S. Navy meteorological staff at several manned stations, including Byrd (80°S, 120°W), Casertz (82.5°S, 117°W), South Pole, and

TABLE 1. Summary of pilot balloon launches at Upstream B and South Camp.

	Camp site	
Hour (LST)	Upstream B No. of observations	South Camp No. of observations
0900	11	20
1200	11	10
1500	22	20
1800	8	6
2100	14	19

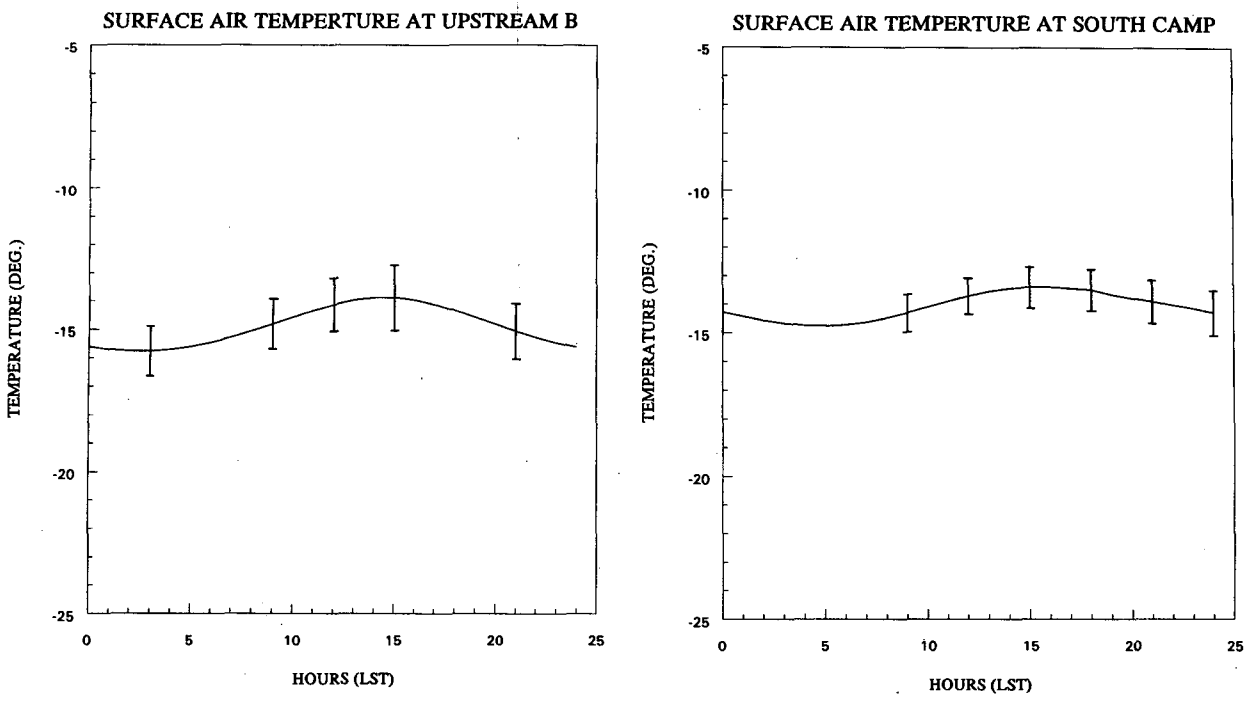

FIG. 5. Average diurnal variations of surface air temperature observed from 11 November to 8 December 1992 for (a) Upstream B, (b) South Camp. Data availability for the monitored hours at both sites exceeds 90%. Standard errors for the monitored hours are plotted as error bars. The unobserved hours are 0300 and 0600 LST at South Camp and 0000, 0600, and 1800 LST at Upstream B. An interpolation scheme, described in section 2, was used to infer the missing values.

from some automatic weather stations (AWS, marked in Fig. 4) over the Ross Ice Shelf (Keller et al. 1994) were used to generate a composite wind and potential temperature analysis. Cloud-cover analysis was performed based upon the surface observations from the manned stations. Advanced Very High Resolution Radiometer (AVHRR) visible images from National Oceanic and Atmospheric Administration (NOAA) polar-orbiting meteorological satellites provide additional information on cloud cover and distribution over all of West Antarctica. Unfortunately, only the system at McMurdo Station (Van Woert et al. 1992) was operational during the field season [the other is located at Palmer Station (65°S, 64°W)], which means that the satellite imagery offers better coverage in the western part of West Antarctica than in the eastern part. The satellite images of 1.1-km resolution at nadir were processed on a workstation using the TeraScan Software Package developed by SeaSpace.

b. Data averaging

In order to examine the average diurnal variation of ABL winds and temperatures, temporal averaging is applied to surface observations and sodar winds. Due to logistic limitations, the field program, which lasted nearly one month, was relatively short in comparison to similar programs in the midlatitudes. This situation is typical of Antarctic ABL studies, for example, a similar project was conducted for one month along the slope of Adélie Land, East Antarctica (Kodama et al. 1989). During the field program, fair weather and partly cloudy skies prevailed. There were two events (each lasting less than 48 h) in which synoptic and mesoscale disturbances significantly influenced the ABL winds and temperatures. These two events will be addressed separately in two other papers. The spatial distribution of the temporally averaged surface potential temperature, which will be presented in the next section, resembles the annual analysis given by Radok (1973). Therefore, this approach is capable of filtering out most synoptic and mesoscale influences and has been used in other ABL studies. For example, Kodama et al. (1989) used this method to examine the average diurnal variation of ABL winds and temperatures along the Adélie Land slope. Also, May and Wilczak (1993) used monthly averages of the daily wind and temperature fields measured from wind profilers and RASS to study ABL diurnal and seasonal variations.

3. Surface observational analysis

a. Winds and temperatures

Averages of surface temperatures and winds (speed and direction) throughout the day at both sites are shown in Figs. 5 and 6. Diurnal temperature ranges

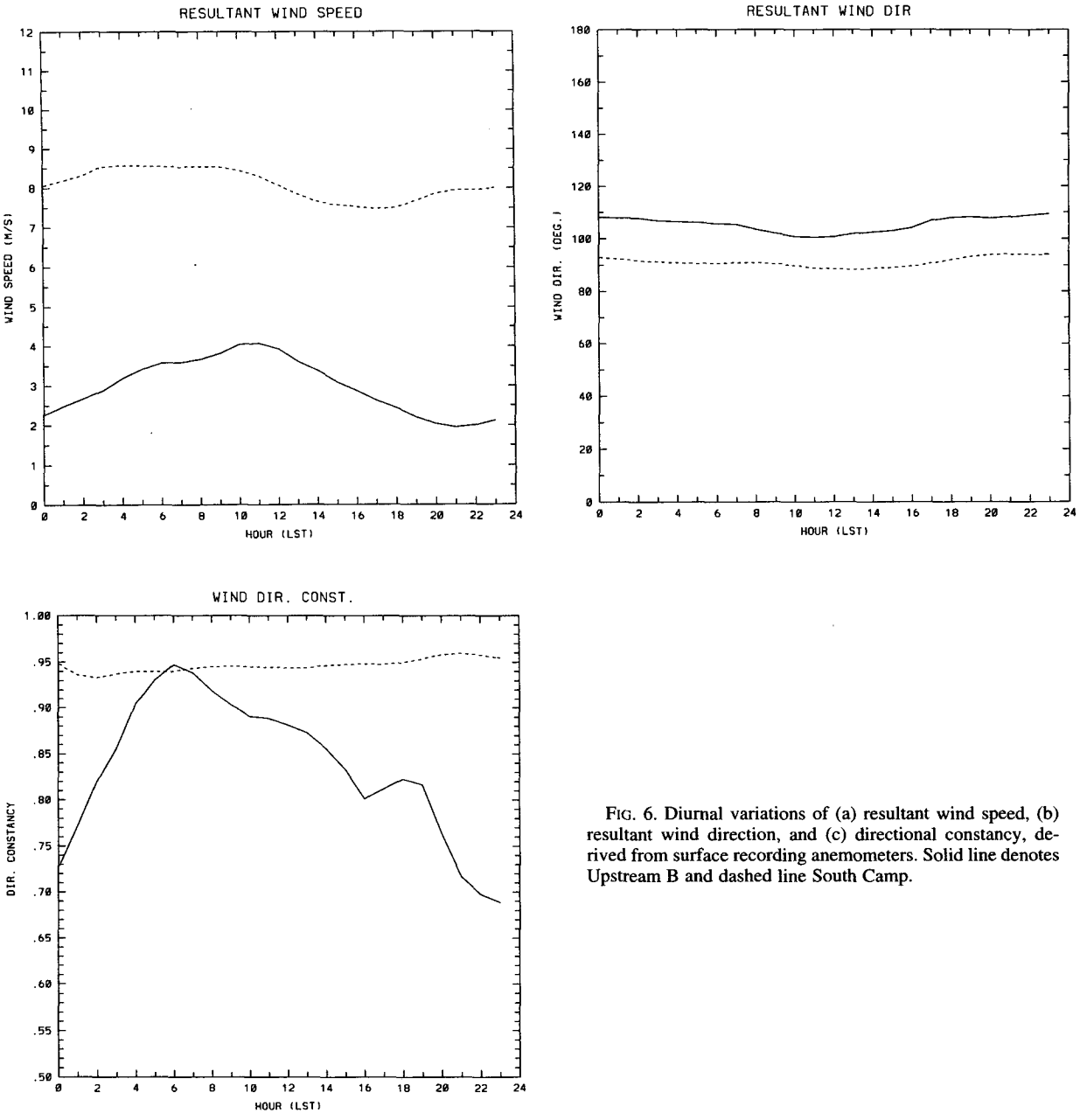

FIG. 6. Diurnal variations of (a) resultant wind speed, (b) resultant wind direction, and (c) directional constancy, derived from surface recording anemometers. Solid line denotes Upstream B and dashed line South Camp.

(Fig. 5) are 1.9°C at Upstream B and 1.4°C at South Camp. These small ranges are mostly due to small variations of local solar elevation (averages: 14°–28° at Upstream B, 15°–27° at South Camp; calculated from Zhang and Anthes 1982). During the field program, the average daily temperature steadily increased by approximately 10°C. Because the solar declination angle only increased around 5° during the field program, the impact of the increased insolation is likely to be small. As described later, the primary cause of this warming is maritime warm-air advection. The sinusoidal temperature curves in Fig. 5 are similar to those observed at D-47 (67.4°S, 138.7°E) in East Antarctica (Kodama et al. 1989) from 20 November to 22 December 1985. The diurnal range at the latter site is much larger (about 9°C) than that at Upstream B, primarily due to the 16° more northerly latitude of D-47. At Upstream B, the diurnal temperature range is slightly larger than that at South Camp (1.9°C versus 1.4°C). There are two factors contributing to this difference if cloud effects can be neglected (see below). First, South Camp is located about 110 km to the south of Upstream B and has a slightly smaller diurnal variation of solar elevation. The second, and probably major factor, is that much higher

wind speeds were generally observed at South Camp (Fig. 6a); these created stronger downward turbulent heat flux than at Upstream B to compensate the longwave radiational cooling at the surface (Bromwich 1989). The mean surface temperatures are −14.9°C at Upstream B and −14.1°C at South Camp. Assuming a generally representative lapse rate along the snow surface of 9.8°C km^{-1} (Radok 1973), South Camp is about 3.7°C warmer than it should be based on its 296-m greater elevation than Upstream B. The strong wind speeds at South Camp partially contribute to the warming. Another factor is warm air advection over South Camp, which will be described in the next section. The maximum and minimum temperatures at Upstream B appear 2–3 h earlier than those at South Camp.

Surface wind speeds at both sites (Fig. 6a) also show diurnal variations with the wind speed maximum occurring in the morning and the speed minimum in the evening. The resultant wind speed range at South Camp is smaller than that at Upstream B. Figures 6a and 6c show that the resultant wind speeds and wind directional constancies at South Camp are much higher than those at Upstream B. High directional constancy is maintained throughout the day at South Camp (Fig. 6c), which is also reflected in the very small diurnal resultant wind direction change (Fig. 6b); by comparison at Upstream B, high directional constancy only appears during the high wind speed period in the morning and a noticeable wind direction change occurs during the day.

Comparing Fig. 6a with Fig. 5, the minimum wind speeds at both sites occur after the maximum temperatures appear. It is also noticeable that the maximum wind speeds at both sites do not appear soon after the minimum surface air temperatures. Kodama et al. (1989) described locally generated katabatic winds where the wind maximum occurred shortly after the minimum temperature. In Fig. 6a, the period of maximum wind at South Camp lasts from approximately 0300 to 0900 LST. The starting time is earlier than the minimum temperature. At Upstream B, the maximum wind occurs at 1100 LST, which is much later than the minimum temperature. These results question whether or not the drainage flow at both sites is locally generated. To examine this, the local downslope buoyancy force ($g\delta\theta\alpha/\theta$) is examined, where g is the gravitational acceleration, $\delta\theta$ the inversion strength, θ the mean potential temperature in the boundary layer, and α the slope angle. Knowing the downslope buoyancy force, the corresponding katabatic wind can be estimated from the equation used by Ball (1960) to calculate katabatic winds over the ice slopes of Antarctica. From RASS, Air-Sonde balloons, and surface observations, the mean inversion strengths are approximately 1.9 K at South Camp and 3.7 K at Upstream B. The mean potential temperatures are 267.7 K at South Camp and 263.5 K at Upstream B. Using the slopes given earlier and these values, the equation (Ball 1960) yields katabatic wind speeds of 1.2 m s^{-1} at South Camp and 0.7 m s^{-1} at Upstream B. These wind speeds show that it is impossible to locally generate the observed katabatic wind speeds (Fig. 6a).

An analysis of winds and temperatures was constructed for Siple Coast and surrounding areas, including the Ross Ice Shelf and the South Pole. Unlike the AWS over the Ross Ice Shelf, manned stations like Byrd (elevation 1530 m) and Casertz (elevation 1457 m) do not have continuous surface observations. Based on the times with most available data, analyses for 0900 LST (in the Upstream B area) and 2100 LST are shown in Figs. 7a and 7b. From Fig. 7, it can be seen that the winds at Byrd and Casertz are blowing (converging) toward the Transantarctic Mountains. Wind speeds over West Antarctica and the Ross Ice Shelf do not change significantly from 0900 to 2100 LST except at Upstream B where wind speed decreases by 2.5 m s^{-1} at 2100 LST. One marked feature in both Figs. 7a and 7b is that the wind speed increases from Upstream B to South Camp, which has been described above. This confirms that a confluence zone exists in the Siple Coast area.

Based on the above results, it is concluded that South Camp, throughout the day, is situated in the katabatic wind confluence zone where surface winds are strong and persistent. By contrast, Upstream B is close the edge of the confluence zone and less affected by it. As the upstream katabatic airflow intensifies in the morning, the katabatic wind confluence zone becomes wider and expands to the north. As the result, the wind speed at Upstream B increases. During the afternoon, the upstream katabatic flow subsides and the confluence zone retreats to the south, resulting in the decreased wind speed. Because the wind speeds at both sites depend on those upstream, the observed maximum winds at both sites do not necessarily occur shortly after the local minimum temperatures. Note that only a small change in the upwind conditions may be required to produce the marked impact at Upstream B because it is located close to the edge of the confluence zone (Bromwich 1986).

At 0900 LST (Fig. 7a), surface potential temperatures over West Antarctica are warmer than those over the Ross Ice Shelf. This is partly because the solar elevation angle over West Antarctica is higher than that over the Ross Ice Shelf. At 2100 LST, the solar elevation angle over the Ross Ice Shelf is higher than that over West Antarctica. Figures 7a and 7b show that the surface potential temperatures fall only slightly over West Antarctica but increase several degrees over the Ross Ice Shelf. One important feature found in both figures is that the surface potential temperatures are much higher at Byrd and Casertz than those at South Camp and Upstream B. This feature is present in the annual mean surface potential temperatures (Radok 1973). This suggests that the length of the field program, though short in comparison with its counterparts in midlatitudes, is capable of representing climatological conditions.

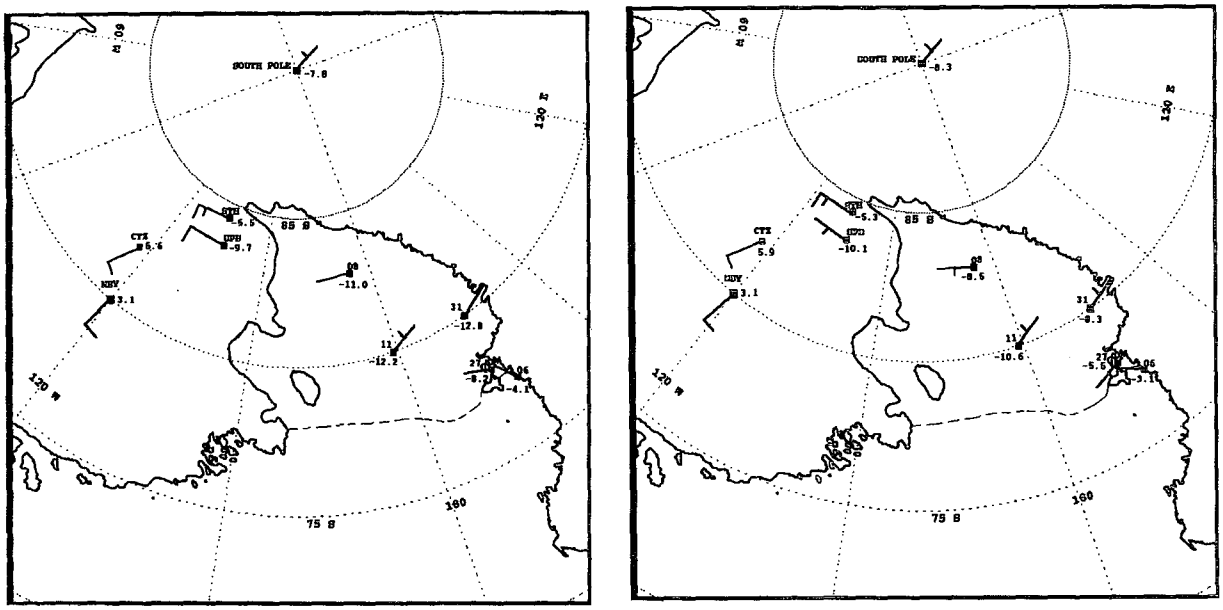

FIG. 7. AWS and manned observational analyses of surface resultant wind and potential air temperature (°C) for the period from 11 November to 8 December 1992. Winds are plotted using conventional notation: (a) 0900 LST, (b) 2100 LST.

b. *Cloud cover analysis*

Cloud cover analysis has been performed based on the surface observations from the manned stations. Averages of total cloud cover for Byrd, Casertz, Upstream B, and South Camp are $^{6}/_{10}$, $^{4}/_{10}$, $^{4}/_{10}$, and $^{3}/_{10}$ at 0900 LST and $^{6}/_{10}$, $^{5}/_{10}$, $^{3}/_{10}$, and $^{3}/_{10}$ at 2100 LST. These averages reveal that the cloud cover basically decreases from north to south and from east to west. The cloud cover analysis has been extended to all of West Antarctica by using the AVHRR images described earlier in section 2. Images at 0900 and 2100 LST were used for the analysis. Availability of the images area ranges from 75% to 8% of the possible total during the field season. The availability decreases from west to east with at least of 50% of images available along and to the west of a line between 75°S, 125°W and 85°S, 95°W. Figure 8 shows the isolines of total cloud cover over West Antarctica. First, the results are quite consistent with the above analysis based upon the surface observations from the manned stations. Second, cloud cover decreases from Ellsworth Land (marked in Fig. 4) to Siple Coast. Third, a strong gradient appears on the west side of the terrain crest. Such a distribution implies the influence of warmer and moister maritime air masses resulting from the marked influence of synoptic forcing to the north of Casertz. These air masses bring in moisture in the form of clouds and precipitation. A heat balance study in East Antarctica showed that a more positive radiation budget (more downwelling longwave radiation) accompanies increased cloudiness (Wendler et al. 1988). Therefore, more clouds over Byrd and Casertz contribute to their warmer surface temperatures.

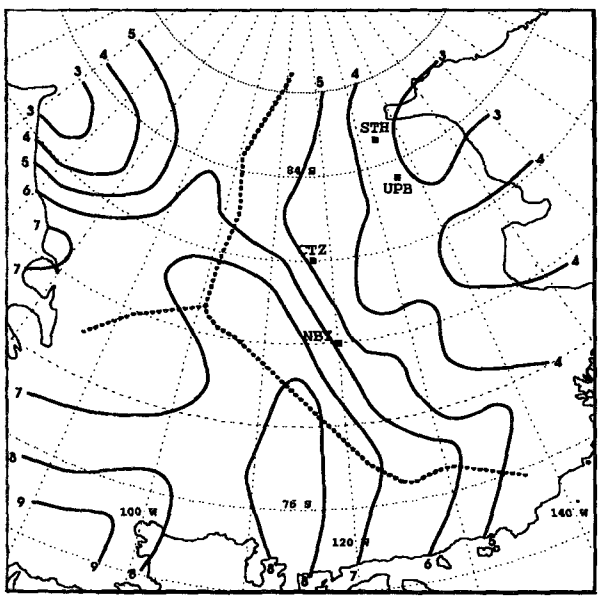

FIG. 8. Mean cloud cover (unit: tenths) analysis derived from the NOAA AVHRR images (7 November 1992–8 December 1992). Dashed line marks the crest of the terrain.

c. *East Antarctic katabatic flow*

The potential temperature is a particularly effective tracer of the near-surface air masses due to the low

absolute humidity environment. The marked temperature contrasts in Fig. 7 suggest the following situation: a much colder (in comparison to that at Byrd and Casertz) katabatic flow coming from East Antarctica influences South Camp and Upstream B because the potential temperature at South Pole approximates that at the two sites. A more buoyant katabatic flow from West Antarctica, which is strongly affected by maritime influences, converges into the Siple Coast area and probably overrides the cold katabatic flow from East Antarctica. The propagation of the cold katabatic flow from East Antarctica is difficult to prove for the time being, at least from the observational point of view, because 1) no data are available from the triangular area bounded by Casertz, South Camp, and the South Pole, which would provide crucial information on this cold katabatic flow; and 2) the katabatic airflow from East Antarctica should have little diurnal variation, coming from an area so close to the geographic South Pole.

The relative scarcity of conventional surface weather observations over the West Antarctic ice sheet dictates that the katabatic flows from East Antarctica must be validated primarily by indirect evidence. This consists of evaluations of sastrugi orientations, numerical simulations, and the potential temperature analysis. Sastrugi orientations were observed during oversnow traverses operating out of Byrd Station soon after the International Geophysical Year (1957–58) (Parish and Bromwich 1986). Comparisons between sastrugi orientations and streamlines from numerical simulations have been conducted before. The results show that Parish's numerical simulations agree closely with sastrugi directions on the East Antarctic plateau (Parish 1982; Bromwich and Kurtz 1984) and over West Antarctica (Parish and Bromwich 1986). Therefore, streamline analyses from numerical simulations provide very important indirect evidence to support the East Antarctic katabatic flow. Parish and Bromwich (1986), through investigation of sastrugi observations, concluded that katabatic flow from East Antarctica probably contributes to the Siple Coast confluence zone. Streamline analyses from recent numerical studies of winter katabatic winds from West Antarctica crossing Siple Coast also confirm this possibility (Bromwich et al. 1994).

4. ABL wind and temperature profile analyses

a. Wind profile analysis

In comparison to a conventional sodar, wind data from pilot balloon launches provide more information at higher altitudes. Pilot balloons were launched in daytime hours at both sites (Table 1). Figures 9a, 9b, and 9c, respectively, show the derived horizontal resultant wind speed, resultant wind direction, and directional constancy profiles. A typical katabatic wind pattern (Kodama et al. 1989), with a low-level jet and decreasing wind speed with height, can be seen at both sites. Similar to the analyses presented earlier, the low-level wind speeds at South Camp are nearly twice as strong as those at Upstream B. The low-level jet at South Camp is more pronounced than at Upstream B. The depths of the katabatic airflow are also resolved by Figs. 9a, 9b, and 9c. At Upstream B, the depth is about 1500 m AGL where the minimum wind speed and directional constancy occur and where the wind direction abruptly switches by 180°. However, at South Camp, the depth is more than 2000 m AGL. The variability of wind direction near 1500 m at Upstream B (Fig. 9b) occurs because the depth of the katabatic flow changes. This is also reflected in the directional constancy profile by the small values. Resultant wind speeds at South Camp are greater than those at Upstream B below 1800 m AGL. As mentioned earlier, the presence of the nearly east–west-oriented Transantarctic Mountains, which are located south of South Camp with an average elevation of about 2500 m, plays an important role in contributing to the depth and wind speed differences. In general, the Coriolis-induced concentration of mass transport on the left side (looking downwind) of the confluence zone is blocked up against the mountains, resulting in the depth difference. At Upstream B (Fig. 9b), the wind direction change with height below 1500 m is small. At South Camp, the wind direction also varies little with height.

As shown in Fig. 6a, the diurnal variation of surface wind is small at South Camp in comparison with that at Upstream B. Therefore, it is inferred that the diurnal variation of ABL wind at South Camp is small. In section 3, it is indicated that the comparatively large diurnal variation of the surface wind at Upstream B is due to the expansion and contraction of the confluence zone. To obtain a better picture of this variation, the katabatic flow components (U, V), as a function of local standard time, are derived from the continuously running sodar at Upstream B. Figures 10a, 10b, and 10c, respectively, show the hourly average sodar U, V, and directional constancy profiles. Comparison between Figs. 10a and 10b shows that the U component is dominant. The low-level jet is better resolved in Fig. 10a than by the balloon launches. The intensity of the low-level jet varies during the day (Fig. 10a): the maximum occurs in the early morning and the minimum near the midnight. The diurnal variation of the jet intensity represents the north–south movement of the confluence zone: in the morning (afternoon), the zone moves north (south) and results in the wind speed increase (decrease). The wind directional constancy also supports the zone movement. Figure 10c shows that high (low) wind directional constancy accompanies the maximum (minimum) wind speed. The high directional constancy is associated with the northward movement of the confluence zone since a similar situation is found at South Camp. When the zone retreats to the south, lighter and more variable winds result in lower directional constancies. The zone movement also

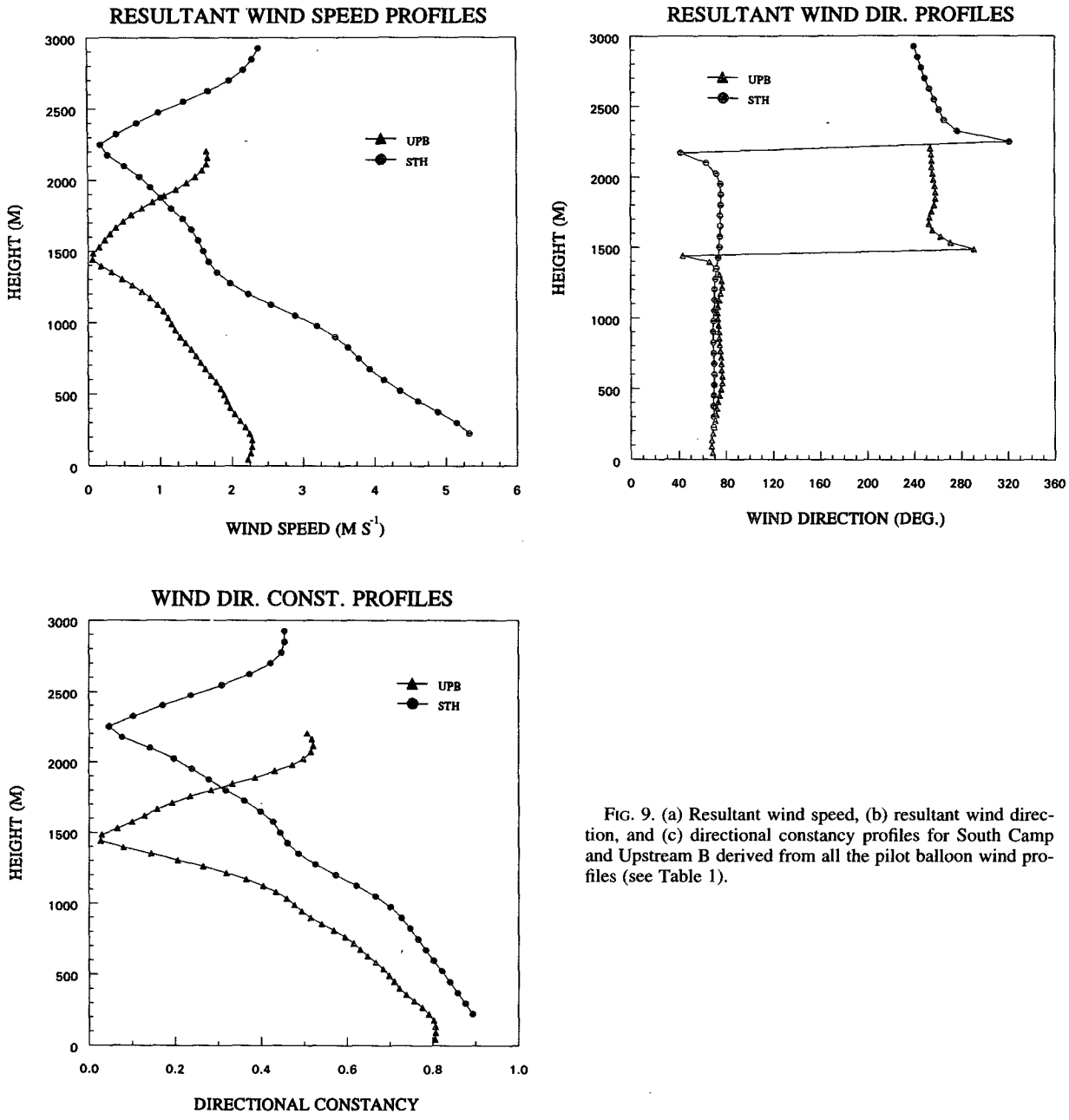

FIG. 9. (a) Resultant wind speed, (b) resultant wind direction, and (c) directional constancy profiles for South Camp and Upstream B derived from all the pilot balloon wind profiles (see Table 1).

causes the jet to rise in the early morning and to descend near midnight. Because the intensity of the low-level jet greatly exceeds that of the locally generated katabatic wind, it is concluded that Upstream B is situated in the confluence zone for most of the day. Comparing Fig. 10a with the surface resultant wind speed (Fig. 6a), it is found that the times when the maximum wind speeds occur are different between the surface and the ABL. At the surface, the maximum wind occurs at 1100 LST, which is several hours after the ABL maximum. This difference may be caused by the propagation of the surface wind from an anomalous upstream origin and its arrival at Upstream B around noon. To confirm this, a network of AWS is required, which is further discussed below.

b. Temperature profile analysis

The temperature profile analysis is based on RASS and Air-Sonde data described in section 2. The temperature profiles at South Camp, measured by the Air-Sonde launches, show a large variation in the ground-

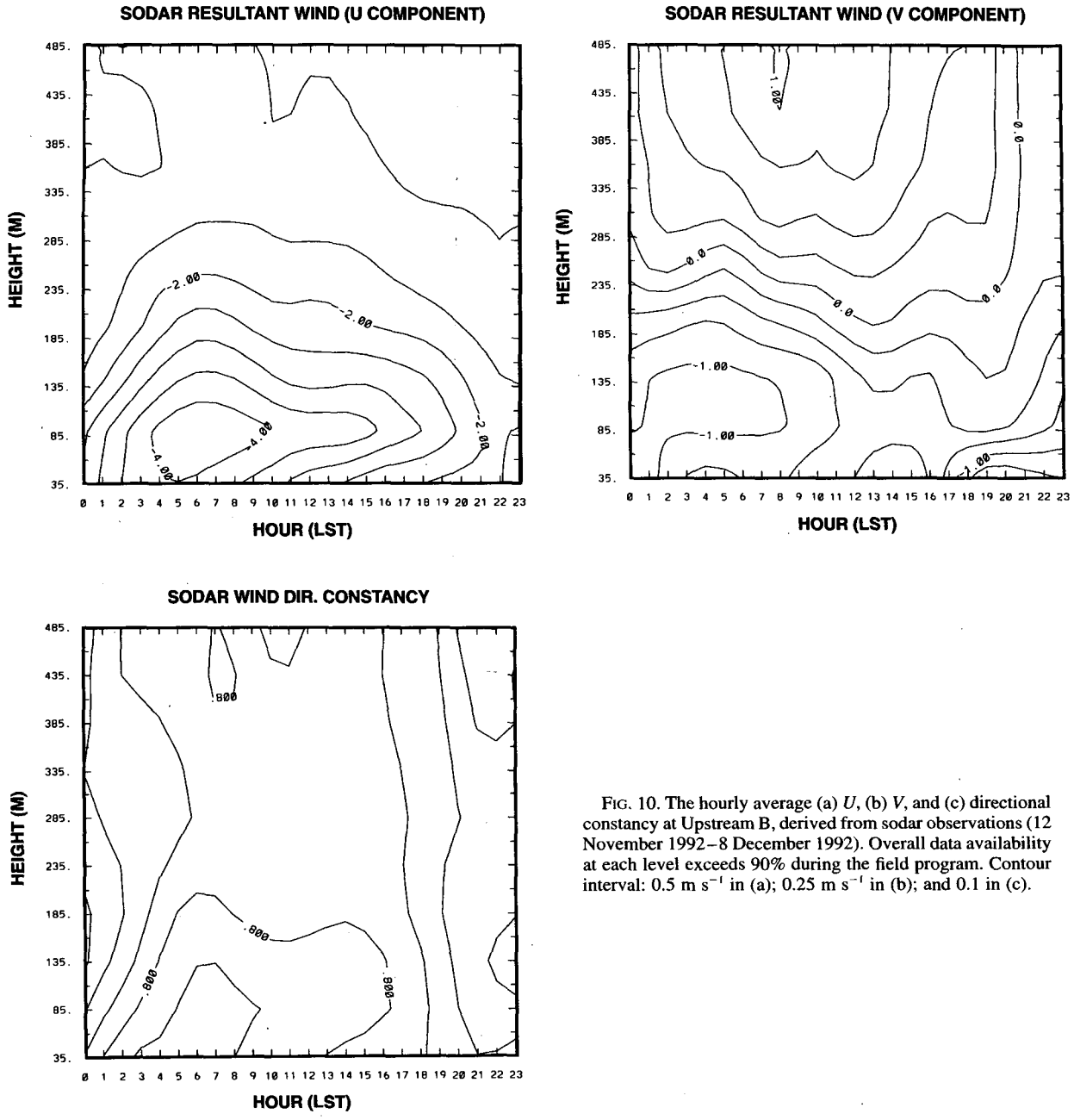

FIG. 10. The hourly average (a) U, (b) V, and (c) directional constancy at Upstream B, derived from sodar observations (12 November 1992–8 December 1992). Overall data availability at each level exceeds 90% during the field program. Contour interval: 0.5 m s^{-1} in (a); 0.25 m s^{-1} in (b); and 0.1 in (c).

based mixing layer and the inversion-layer heights. Despite this large variation, the profiles show a consistent pattern. Figure 11 shows a typical temperature profile observed at 1500 LST. Of the 23 profiles observed daily at 1500 LST, 21 (91% of the total) were found to have this pattern. In Fig. 11, the ground-based, nearly adiabatic lapse rate is associated with the mechanical mixing layer due to the strong wind (13 m s^{-1}, measured at the low-level jet) blowing over the well-developed sastrugi field described in section 2. This suggests that mechanical mixing dominates the lower ABL. A convective layer caused by heating from the snow surface, due to shortwave radiation absorption, is at best very weakly developed. This is significantly different from that observed in East Antarctica (Kodama et al. 1989) where the ground-based convective boundary layer prevails. Another prominent feature shown in Fig. 11 is that an inversion layer overlies the low-level mixing layer. The average inversion strength, measured from the top of the low-level mixing layer to the top of the lifted inversion layer, is 1.9°C (σ = 1.3°C), based on the 21 daily observations. The

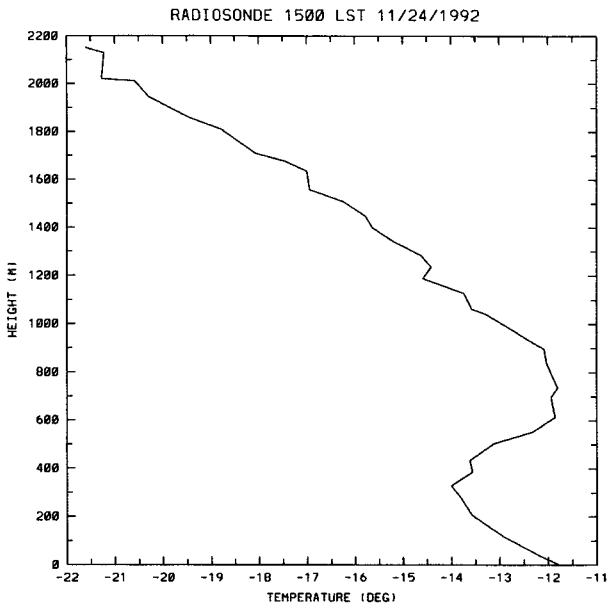

FIG. 11. Representative temperature profile at South Camp, measured by Air-Sonde flight at 1500 LST 24 November 1992.

presence of the inversion layer suggests that warm-air advection is present above South Camp. In section 3, the possible existence of warm advection is mentioned based on the analyses of surface winds and temperatures in the confluence zone and its surrounding areas. The ABL temperature profile analysis provides additional evidence for the existence of warm-air advection.

Unlike the sodar, the RASS experienced more problems in the Antarctic environment. The maximum measurement height was severely limited due primarily to the lack of moisture. Detailed discussions can be found in May and Wilczak (1993) and Kaimal and Finnigan (1994). Measured RASS temperature profiles at Upstream B were scattered during the field program. Similar to the temperature profile at South Camp, the measured RASS temperature profiles also have a consistent pattern. Figure 12 shows a typical RASS temperature profile measured at 2300 LST. The profile shows a weak inversion layer extending from the surface to around 400 m AGL. Comparing this profile with that at South Camp (Fig. 11), it is found that the mechanical mixing layer does not appear in this profile. This is because of the absence of strong winds and a rough surface at Upstream B, which are the necessary conditions for the mechanical mixing. As indicated in section 3, the diurnal variation of surface temperature at Upstream B is small (approximately 1.9°C). Therefore, the diurnal variation of the ABL temperature profile can be inferred to be small.

5. Synthesis

A month-long field program to study the springtime katabatic wind confluence zone has been carried out near Siple Coast, West Antarctica. In comparison to its counterparts in East Antarctica (Bromwich et al. 1993), the Siple Coast confluence zone shares many similarities. Due primarily to the Coriolis-induced concentration of mass transport on the left side (looking downwind) of the confluence zone as well as to the adjacent Transantarctic Mountains that deflect airflow into the Siple Coast area and result in mountain blocking, the ABL winds and temperatures vary greatly inside the confluence zone. The surface wind speed and directional constancy, on average, increase markedly from north to south. South Camp in general is inside the strong wind zone, which results in higher wind speeds (nearly twice those at Upstream B) and directional constancies. Upstream B, on the other hand, is farther away from the Transantarctic Mountains and therefore less affected by the strong wind zone, resulting in lower wind speed. This factor also makes Upstream B more easily exposed to other influences, such as local katabatic flow, which partially contributes to the lower average directional constancy. Strong low-level mixing created by strong winds over the rough sastrugi field also makes the surface temperature at South Camp warmer than that at Upstream B. The surface air temperatures and the katabatic winds at both sites show weak diurnal variations. The diurnal ranges are larger at Upstream B than at South Camp.

Above the surface level, low-level jets are observed at both sites, but the jet at South Camp is well-defined and nearly twice as strong as that at Upstream B. The near surface thermal structure of the boundary layer at South Camp was modified by the presence of strong winds. An inversion layer overlies this mixing layer,

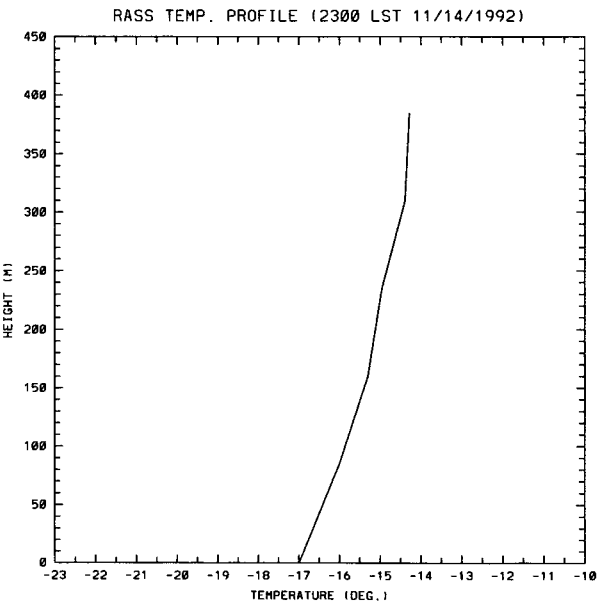

FIG. 12. Representative temperature profile at Upstream B Camp, measured by RASS at 2300 LST 14 November 1992.

which implies the presence of warm-air advection. By contrast, at Upstream B, the boundary layer thermal structure mostly relies on the weak warm-air advection. Also, the lack of strong winds is an additional factor allowing moderate stratification to develop. As a result, during this campaign period, the inversion strength is rather weak, as is the diurnal variation of surface temperature. However, from the temperature profile analysis at both sites, the average inversion tops extend to about 500 m AGL.

At Upstream B, the diurnal variation of the katabatic flow is noticeable: high (low) wind speeds are found in the morning (evening). The wind directional constancy also follows the same trend. This is another contributor to the much smaller average directional constancy in comparison to that at South Camp. Based on the surface and sodar wind analyses, it is shown that the confluence zone becomes wider in the morning because the upstream converging katabatic flow becomes stronger due to diurnal cooling. Detailed explanations of the inversion layer and the diurnal variation of the katabatic flow are related to the heat balance of the snow surface. These require measurements of radiation fluxes, as well as those of sensible and latent heat, which were not carried out during the field program. Therefore, the following discussion has to rely on past observations from East Antarctica. At the South Pole, surface energy balance study (Carroll 1982) indicates that downward heat flux from the air exceeds surface net radiation losses during summer. For lower-latitude areas, net radiation studies (Rusin 1964) at Vostok (78.5°S, 106.8°E) and Komsomolskaya (74.1°S, 97.5°E) show that typically there is a period (10–11 h) of negative radiation budget during each day. In a study of the surface heat balance at D-47 [same time and location as the study by Kodama et al. (1989)], Wendler et al. (1988) concluded that the sensible heat flux remained downward for most of the day, which means that the air above the surface was cooled and an inversion was maintained. Even during the short period of upward sensible heat flux, the drainage flow was still present probably because of a background temperature gradient associated with the land versus ocean contrast (Kodama et al. 1989). This also explains why high directional constancy persists throughout the day. A summertime numerical simulation (Parish et al. 1993) indicated that the katabatic wind is a robust feature of the Antarctic boundary layer. Therefore, the observed inversion-layer behavior and the modest diurnal variation of the katabatic flow can be explained by the following. Because upward heat flux from the surface decreases the inversion strength during periods with high solar elevation, the katabatic flow, as a response, also weakens. During the low solar elevation period, the sensible heat flux becomes downward, and thus, the inversion strength increases along with the katabatic flow.

The composite analyses of surface observations provide additional confirmation for the existence of the Siple Coast confluence zone. The analysis of the wind field indicates that air currents from the interior converge into the Siple Coast area. The analysis of the potential temperature field indicates that warm (cold) temperatures appear in the areas of high (low) elevation in West Antarctica. The cloud analysis, which shows that more (less) clouds appear in the warm (cold) areas, suggests greater maritime influence in the high elevation areas near Byrd and Casertz. This, in combination with the wind field analysis, supports the contention that warm katabatic flow from the West Antarctic interior overlies a cold katabatic flow from East Antarctica.

Parish and Bromwich (1986), through analysis of sastrugi observations collected during separate summers, addressed the likelihood that katabatic flow from East Antarctica contributes to the Siple Coast confluence zone. Streamline analysis from recent numerical study of winter katabatic winds from West Antarctica crossing Siple Coast confirms this possibility (Bromwich et al. 1994). Additional evidence for such a scenario comes from a case study of a mesoscale cyclone occurring during the campaign (Smith et al. 1993; Carrasco 1994). Based on past mesoscale cyclogenesis studies at Terra Nova Bay and near the foot of Byrd Glacier (Bromwich 1991; Carrasco and Bromwich 1993), a surface-based baroclinic zone is an essential ingredient for mesoscale cyclogenesis. Such a baroclinic zone can form where the northern edge of the cold East Antarctic katabatic flow meets the edge of the warmer katabatic flow from West Antarctica. The case study (Smith et al. 1993; Carrasco 1994) implies the existence of such baroclinic zone during the mesoscale cyclone development. Indirect support for this hypothesis is provided by Carrasco and Bromwich (1994), who noted for 1988 that mesoscale cyclones often moved from West Antarctica across Siple Coast to the Ross Ice Shelf. Because Siple Coast was near the edge of their investigation area, no detailed evaluation of the genesis mechanisms was undertaken. The strongest evidence for the persistent presence of this feature is provided by the year-long (1991) satellite study of mesoscale cyclogenesis by Carrasco (1994), which resolved a strong maximum of mesoscale cyclogenesis in the area of the inferred baroclinic zone.

The controlling dynamics can be summarized as follows. Bromwich et al. (1994) evaluated the force balance associated with simulated winter katabatic winds from West Antarctica crossing Siple Coast and the Ross Ice Shelf. The analysis for the Siple Coast area showed that the downslope buoyancy force dominated. The analysis over the Ross Ice Shelf indicated that a barrier wind is formed along the Transantarctic Mountains. The governing dynamics of this barrier wind are described by Bromwich et al. (1994) as follows. When a katabatic wind blows down onto the flat ice shelf, it

immediately loses the downslope buoyancy forcing. The Coriolis force turns the flow to the left over the almost frictionless ice shelf and eventually reaches the mountains, where it must pile up because the stratified flow cannot surmount such a vertical wall. Geostrophic balance is established between the Coriolis force and the restoring force associated with the blocking. This barrier wind is also called a katabatic forced barrier wind (Bromwich et al. 1994). In the summer, the inversion strength in Siple Coast is markedly reduced. The field measurements (presented earlier) show that the inversion strength in Siple Coast was reduced from an estimated 15°C in the winter (see Fig. 2.5 in Schwerdtfeger 1984) to less than 4°C. The calculation given in section 3a demonstrates that the downslope buoyancy force in the Siple Coast area is no longer the dominant force during summer. Therefore, the summer situation resembles that for the katabatic winds propagating over the Ross Ice Shelf in winter, except that the airflow blocking against the Transantarctic Mountains only exists in the West Antarctic katabatic wind component (whose depth varies in the north–south direction) and the wind speeds are reduced. This also suggests that the barrier wind regime moves upstream to the Siple Coast area. As discussed previously, the role of the Transantarctic Mountains is to deflect the Coriolis-induced concentration of mass transport, which is on the left side (looking downwind) of the confluence zone, into the gently sloping Siple Coast area and to form a West Antarctic barrier wind parallel to the mountains. The East Antarctic katabatic wind component is not blocked by the Transantarctic Mountains because it blows away from the mountains and the flow depth does not change along the sloping terrain (section 4). However, this East Antarctic wind component is influenced by the presence of the West Antarctic barrier wind aloft and the downslope buoyancy force associated with the cold air over the sloping terrain.

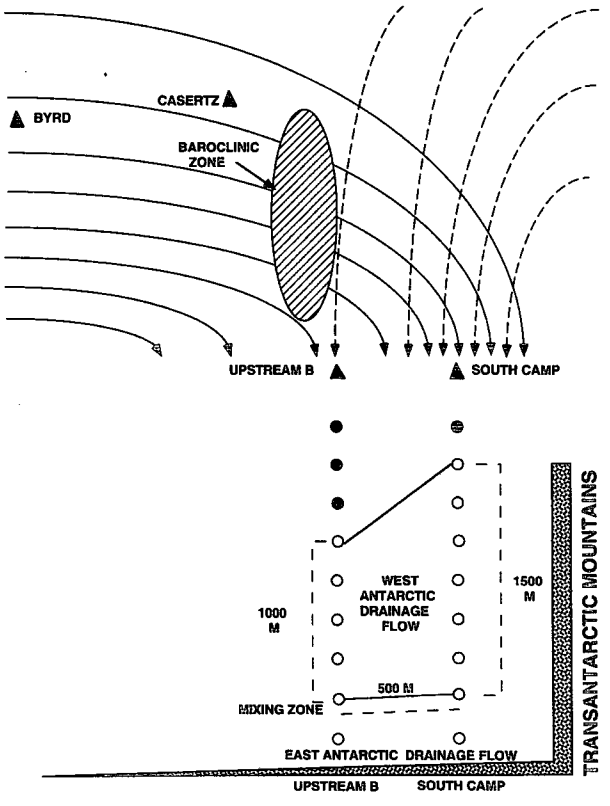

FIG. 13. Schematic illustration (plan view) of the katabatic wind confluence zone near Siple Coast, West Antarctica, is given at top. The solid lines are the streamlines of the surface winds from West Antarctica, and the dashed lines are those of the easterly winds from East Antarctica, which because they are colder undercut the more maritime-influenced flow from West Antarctica. Hatched area shows the baroclinic zone where the two drainage flows meet. Filled triangles are manned stations. At bottom, the north–south cross section from Upstream B Camp to South Camp shows the drainage flow overlap with the West Antarctic component blocked against the Transantarctic Mountains. Open circles denote easterlies (normal to the cross section), and filled circles denote westerlies.

Combining the analyses of the surface composite and of the wind and temperature profiles, the following picture (Fig. 13) for the cross-sectional structure of the confluence zone emerges: 1) the relatively cold katabatic flow, which probably comes from East Antarctica, occupies the layer between the surface and roughly 500 m AGL; 2) low-level jets are present below 200 m AGL and are stronger near the Transantarctic Mountains; 3) diurnal variation exists in this cold katabatic flow and decreases toward the Transantarctic Mountains; 4) weak inversion layer tops are found near 500 m AGL, inferred from the temperature profiles at both sites, which is roughly equal to the depth of the cold katabatic flow; 5) the warmer West Antarctic katabatic flow overlies the cold katabatic flow and has a depth of approximately 1000 m at Upstream B and at least 1500 m at South Camp due to blocking against the Transantarctic Mountains as a result of the West Antarctic airflow convergence; and 6) a baroclinic zone is present where the cold and warm katabatic flows are horizontally adjacent, and this can become unstable and form mesoscale cyclones. Finally, it should be noted that the dashed streamlines in Fig. 13, which outline the propagation of the cold katabatic airflow from East Antarctica, are conjectural and require observational verification.

There are several remaining questions to be answered by future observational and numerical studies. First, a network of surface-based AWS is required to better understand the katabatic components that have different densities; this was established during the 1994–95 austral summer. These AWS will also help to resolve the inferred baroclinic zone and further explain the associated mesoscale cyclogenesis and its interaction with the katabatic winds. Second, observations involving aircraft, such as conducted near Terra Nova Bay in East Antarctica (Parish and Bromwich

1989), are highly desirable to confirm the inferred wind and temperature structure of the confluence zone. As presented above, the dynamics of the Siple Coast confluence zone is quite different and perhaps more complicated than those in East Antarctica. Finally, additional numerical study involving the effects of clouds and warm-air advection is desirable to describe the observed data and illuminate the dynamics governing the behavior of the katabatic flow components.

Acknowledgments. This field program and research were supported by National Science Foundation Grants OPP-8916921 and OPP-9218949 to the first author. Sander Tweeuwisse processed the radiosonde and pilot balloon data. Shawn Smith and Sander Teeuwisse participated in the 1992 campaign along with the authors. Surface weather data at Byrd, Casertz, and the South Pole were provided by the U.S. Navy Meteorological Center at McMurdo Station. AWS data were obtained from Charles R. Stearns of the Department of Atmospheric and Oceanic Sciences at the University of Wisconsin—Madison (NSF Grants DPP 8606385, 8818171, 9015586, and 9303569). The satellite imagery were recorded by the U.S. Navy personnel at McMurdo Station and obtained from Robert Whritner of the Arctic and Antarctic Research Center at Scripps Institution of Oceanography (NSF Grant DPP-8815818). We thank the personnel from Antarctic Support Associates and the U.S. Navy meteorological staff at Upstream B for providing assistance essential to the successful completion of the campaign. The authors also appreciate the substantive and thought-provoking comments from the anonymous reviewers, which significantly improved the manuscript.

REFERENCES

Argentini, S., G. Mastrantonio, G. Fiocco, and R. Ocone, 1992: Complexity of the wind field as observed by a sodar system and by automatic weather stations on the Nansen Ice Sheet, Antarctica, during summer 1988–89: Two case studies. *Tellus,* **44B,** 422–429.

Ball, F. K., 1960: Winds on the ice slope of Antarctica. *Proc. of the Symp. on Antarctic Meteorology,* Melbourne, Australia, Pergamon, 9–16.

Bromwich, D. H., 1986: Surface winds in West Antarctica. *Antarct. J. U.S.,* **21,** 235–237.

——, 1989: Satellite analyses of Antarctic katabatic wind behavior. *Bull. Amer. Meteor. Soc.,* **70,** 738–749.

——, 1991: Mesoscale cyclogenesis over the southwestern Ross Sea linked to strong katabatic winds. *Mon. Wea. Rev.,* **119,** 1736–1752.

——, and D. D. Kurtz, 1984: Katabatic wind forcing of the Terra Nova Bay polynya. *J. Geophys. Res.,* **89,** 3561–3572.

——, T. R. Parish, A. Pellegrini, C. R. Stearns, and G. A. Weidner, 1993: Spatial and temporal characteristics of the intense katabatic winds at Terra Nova Bay, Antarctica. *Antarctic Meteorology and Climatology: Studies Based on Automatic Weather Stations,* Antarctic Research Series, Vol. 61, D. H. Bromwich and C. R. Stearns, Eds., Amer. Geophys. Union, 47–68.

——, Y. Du, and T. R. Parish, 1994: Numerical simulation of winter katabatic winds from West Antarctica crossing Siple Coast and the Ross Ice Shelf. *Mon. Wea. Rev.,* **122,** 1417–1435.

Burden, R. L., and J. D. Faires, 1985: *Numerical Analysis.* PWS-KENT Publishing Co., 676 pp.

Carrasco, J. F., 1994: Dynamics of mesoscale cyclogenesis adjacent to the Pacific coast of Antarctica. Ph.D. dissertation, The Ohio State University, 286 pp.

——, and D. H. Bromwich, 1993: Mesoscale cyclogenesis dynamics over the southwestern Ross Sea, Antarctica. *J. Geophys. Res.,* **98,** 12 973–12 996.

——, and ——, 1994: Climatological aspects of mesoscale cyclogenesis over the Ross Sea and Ross Ice Shelf regions of Antarctica. *Mon. Wea. Rev.,* **122,** 2405–2425.

Carroll, J. J., 1982: Long-term means and short-time variability of the surface energy balance components at the South Pole. *J. Geophys. Res.,* **87,** 4277–4286.

Gallée, H., and G. Schayes, 1994: Development of a three-dimensional meso-γ primitive equation model: Katabatic winds simulation in the area of Terra Nova Bay, Antarctica. *Mon. Wea. Rev.,* **122,** 671–685.

Hall, F. F., and E. J. Owens, 1975: Atmospheric acoustic echo sounding investigations at the South Pole. *Antarct. J. U.S.,* **10,** 191–192.

Hines, K. M., D. H. Bromwich, and T. R. Parish, 1995: A mesoscale modeling study of the atmospheric circulation of high southern latitudes. *Mon. Wea. Rev.,* **123,** 1146–1165.

Kaimal, J. C., and J. J. Finnigan, 1994: *Atmospheric Boundary Layer Flows: Their Structure and Measurement.* Oxford University Press. 289 pp.

Keller, L. M., G. A. Weidner, and C. R. Stearns, 1994: Antarctic automatic weather station data for the calendar year 1992, 380 pp. [Available from Dept. of Atmospheric and Oceanic Sciences, University of Wisconsin—Madison, 1225 W. Dayton St., Madison, WI 53706.]

Kodama, Y., and G. Wendler, 1986: Wind and temperature regime along the slope of Adélie Land, Antarctica. *J. Geophys. Res.,* **91,** 6735–6741.

——, ——, and N. Ishikawa, 1989: The diurnal variation of the boundary layer in summer in Adélie Land, Eastern Antarctica. *J. Appl. Meteor.,* **28,** 16–28.

Liu, Z., and D. H. Bromwich, 1993a: Acoustic remote sensing of planetary boundary-layer dynamics near Ross Island, Antarctica. *J. Appl. Meteor.,* **32,** 1867–1882.

——, and ——, 1993b: A northwesterly wind event near Ross Island. *Antarct. J. U.S.,* **28,** 288–291.

Mastrantonio, G., R. Ocone, and G. Fiocco, 1988: Acoustic remote sensing of the Antarctic boundary layer. *Proc. First Workshop Italian Research on Antarctic Atmosphere,* Bologna, Italy, Italian Physical Society, 137–144.

May, P. T., and J. M. Wilczak, 1993: Diurnal and seasonal variations of boundary-layer structure observed with a radar wind profiler and RASS. *Mon. Wea. Rev.,* **121,** 673–682.

Neff, W. D., 1981: An observational and numerical study of the atmospheric boundary layer overlying the East Antarctic Ice Sheet. NOAA Tech. Memo. ERL WPL-67, 272 pp. [Available from NOAA/Wave Propagation Laboratory, 325 Broadway, Boulder, CO 80304.]

Parish, T. R., 1982: Surface airflow over East Antarctica. *Mon. Wea. Rev.,* **110,** 84–90.

——, and D. H. Bromwich, 1986: The inversion wind pattern over West Antarctica. *Mon. Wea. Rev.,* **114,** 849–860.

——, and ——, 1987: The surface windfield over the Antarctic ice sheets. *Nature,* **328,** 51–54.

——, and ——, 1989: Instrumented aircraft observations of the katabatic wind regime near Terra Nova Bay. *Mon. Wea. Rev.,* **117,** 1570–1585.

——, and ——, 1991: Continental-scale simulation of the Antarctic katabatic wind regime. *J. Climate,* **4,** 135–146.

——, P. Pettré, and G. Wendler, 1993: A numerical study of the diurnal variation of the Adélie Land katabatic wind regime. *J. Geophys. Res.,* **98,** 12 933–12 947.

Radok, U., 1973: On the energetics of surface winds over the Antarctic ice cap. Energy Fluxes over Polar Surfaces, WMO Tech. Note No. 129, 69–100.

Rusin, N. P., 1964: *Meteorological and Radiational Regime of Antarctica.* Israel Program for Scientific Translations, 355 pp.

Schwerdtfeger, W., 1984: *Weather and Climate of the Antarctic.* Elsevier, 261 pp.

Smith, S. R., J. F. Carrasco, and Z. Liu, 1993: A case study of a Siple Coast mesocyclone. *Antarct. J. U.S.,* **28,** 283–285.

Sorbjan, Z., Y. Kodama, and G. Wendler, 1986: Observational study of the atmospheric boundary layer over Antarctica. *J. Appl. Meteor.,* **25,** 641–651.

Stearns, C. R., and G. Wendler, 1988: Research results from Antarctic automatic weather stations. *Rev. Geophys.,* **26,** 45–61.

Van Woert, M. L., R. H. Whritner, D. E. Waliser, D. H. Bromwich, and J. C. Comiso, 1992: ARC: A source of multisensor satellite data for polar science. *EOS, Trans. Amer. Geophys. Union,* **73,** 75–76.

Wendler, G., N. Ishikawa, and Y. Kodama, 1988: The heat balance of the icy slope of Adélie Land, Eastern Antarctica. *J. Appl. Meteor.,* **27,** 52–65.

Zhang, D., and R. A. Anthes, 1982: A high-resolution model of the planetary boundary layer—Sensitivity tests and comparisons with SESAME 79 data. *J. Appl. Meteor.,* **21,** 1594–1609.